

High-order Finite Element Methods on Hybrid Meshes Including Pyramids. Application to Wave Equation and Helmholtz Equation.

M. Duruflé

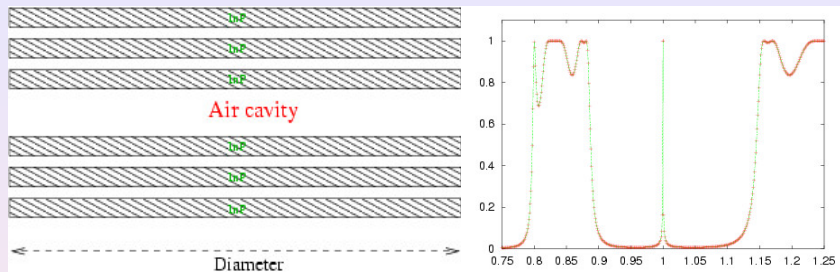
IMB, Bacchus

14th January 2010

Bibliography and motivation

- [S. Fauqueux](#), mixed spectral elements for wave and elastic equations (hexahedra)
- [S. Pernet](#), Discontinuous Galerkin methods for Maxwell's equations (hexahedra)
- [G.E. Karniadakis](#), [S. Sherwin](#), [T. Warburton](#), continuous and discontinuous finite elements on tetrahedra/prisms/pyramids by considering “degenerated” cube
- [Bedrosian](#), Early work on pyramids, nodal basis functions for order 1 and 2
- [Nigam, Philips](#), Recent work on finite element spaces for pyramids, infinite pyramid is the reference element

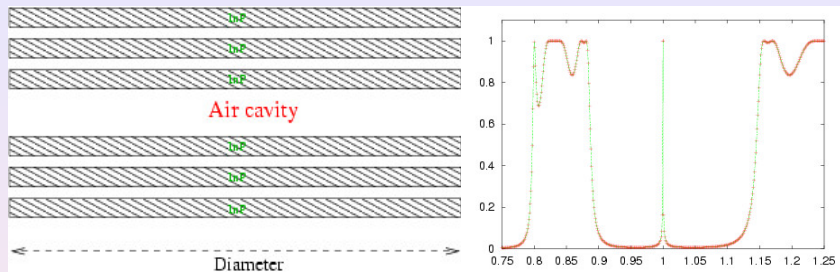
A test case : an optical filter



On the right, transmission coefficient versus frequency

- Frequency $F = 1.0$ is a resonant frequency of the device
- Enlightenment of the device by a gaussian beam.
- PML around the computational domain.

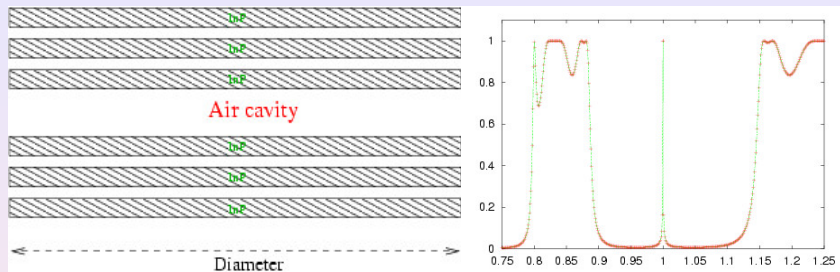
A test case : an optical filter



On the right, transmission coefficient versus frequency

- Frequency $F = 1.0$ is a resonant frequency of the device
- Enlightenment of the device by a gaussian beam.
- PML around the computational domain.

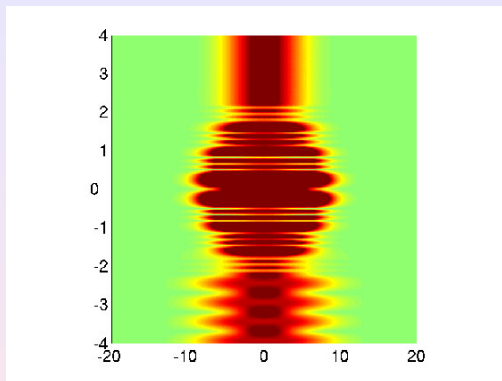
A test case : an optical filter



On the right, transmission coefficient versus frequency

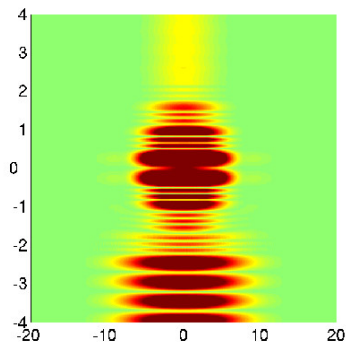
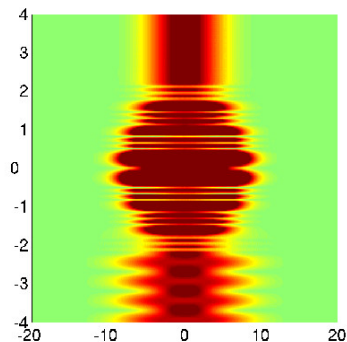
- Frequency $F = 1.0$ is a resonant frequency of the device
- Enlightenment of the device by a gaussian beam.
- PML around the computational domain.

Advantage to use high order method



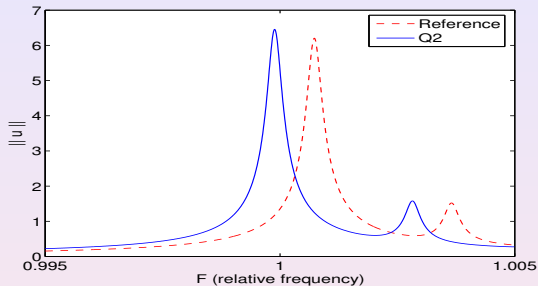
Numerical solution for Q_5 with 10 points by wavelength

Advantage to use high order method



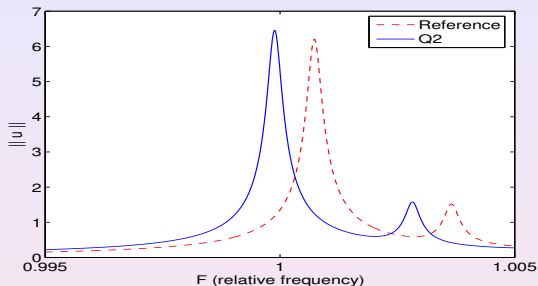
On the right, numerical solution for Q_2 with 10 points by wavelength

Advantage to use high order method



Norm of the solution on the output, according to the frequency

Advantage to use high order method



Norm of the solution on the output, according to the frequency
Which order is optimal to reach an error less than 10% ?

Order	2	3	4	5	6	7
Nb dofs	453 000	69 800	52 000	33 200	47 700	42 200

Helmholtz equation

$$-\rho\omega^2 u - \operatorname{div}(\mu \nabla u) = f \quad \in \Omega$$

Helmholtz equation

$$-\rho\omega^2 u - \operatorname{div}(\mu \nabla u) = f \quad \in \Omega$$

Use of **finite element method** leads to the following linear system :

$$(-\omega^2 D_h + K_h) U_h = F_h$$

Helmholtz equation

$$-\rho\omega^2 u - \operatorname{div}(\mu \nabla u) = f \quad \in \Omega$$

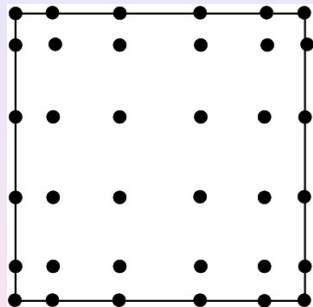
Use of **finite element method** leads to the following linear system :

$$(-\omega^2 D_h + K_h) U_h = F_h$$

Our aim is to develop an efficient iterative solver for an high order of approximation r . Therefore, we need a **fast** matrix-vector product

$$(-\omega^2 D_h + K_h) U_h$$

Elementary matrices



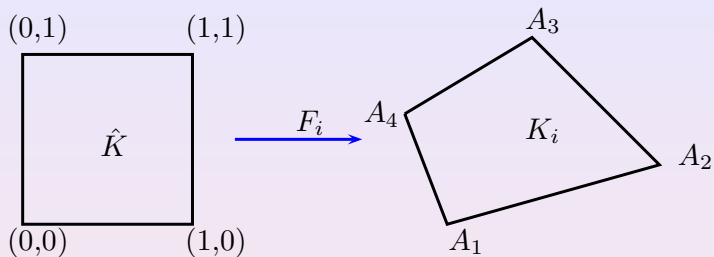
Gauss-Lobatto points for Q_5

on the unit square \hat{K}

Tensorized basis functions :

$$\hat{\varphi}_i = \hat{\varphi}_{i_1}(\hat{x}) \hat{\varphi}_{i_2}(\hat{y})$$

Elementary matrices



The transformation F_i

DF_i, J_i jacobian matrix and determinant

Elementary matrices

$$(D_h)_{i,j} = \int_{\hat{K}} \rho \mathbf{J}_i \hat{\varphi}_i^{GL} \hat{\varphi}_j^{GL} d\hat{x}$$

Use of quadrature formulas (ω_m^X, ξ_m^X) on the unit square/cube

- X can be equal to GL (Gauss-Lobatto quadrature, faster)
- X can be equal to G (Gauss quadrature, more accurate)

Elementary matrices

$$(D_h)_{i,j} = \int_{\hat{K}} \rho \mathbf{J}_i \hat{\varphi}_i^{\text{GL}} \hat{\varphi}_j^{\text{GL}} d\hat{x}$$

Use of quadrature formulas (ω_m^X, ξ_m^X) on the unit square/cube

- X can be equal to GL (Gauss-Lobatto quadrature, faster)
- X can be equal to G (Gauss quadrature, more accurate)

$$(D_h)_{i,j} = \sum_m \omega_m^X \rho \mathbf{J}_i \hat{\varphi}_i^{\text{GL}}(\xi_m^X) \hat{\varphi}_j^{\text{GL}}(\xi_m^X) d\hat{x}$$

Matrix-vector product $D_h U$ can be split into three steps :

$$v_m = \sum_j \hat{\varphi}_j^{\text{GL}}(\xi_m^X) u_j$$

$$w_m = \omega_m \rho \mathbf{J}_i(\xi_m) v_m$$

$$y_i = \sum_m \hat{\varphi}_i^{\text{GL}}(\xi_m^X) w_m$$

Elementary matrices

$$(D_h)_{i,j} = \int_{\hat{K}} \rho \mathbf{J}_i \hat{\varphi}_i^{GL} \hat{\varphi}_j^{GL} d\hat{x}$$

Use of quadrature formulas (ω_m^X, ξ_m^X) on the unit square/cube

- X can be equal to GL (Gauss-Lobatto quadrature, faster)
- X can be equal to G (Gauss quadrature, more accurate)

$$(D_h)_{i,j} = \sum_m \omega_m^X \rho \mathbf{J}_i \hat{\varphi}_i^{GL}(\xi_m^X) \hat{\varphi}_j^{GL}(\xi_m^X) d\hat{x}$$

Underlying factorization

$$\hat{\mathbf{C}}_{i,j} = \hat{\varphi}_i^{GL}(\xi_j^X)$$

$$(\mathbf{A}_h)_m = \omega_m \rho \mathbf{J}_i(\xi_m)$$

$$D_h = \hat{\mathbf{C}} \mathbf{A}_h \hat{\mathbf{C}}^*$$

⇒ only storage of $\omega_m \rho \mathbf{J}_i(\xi_m)$

Elementary matrices

$$(D_h)_{i,j} = \int_{\hat{K}} \rho \mathbf{J}_i \hat{\varphi}_i^{GL} \hat{\varphi}_j^{GL} d\hat{x}$$

Use of quadrature formulas (ω_m^X, ξ_m^X) on the unit square/cube

- X can be equal to GL (Gauss-Lobatto quadrature, faster)
- X can be equal to G (Gauss quadrature, more accurate)

Product $Y = \hat{C}U$ is split into three steps :

$$v_{i_1, j_2, j_3} = \sum_{j_1} \hat{\varphi}_{j_1}^{GL}(\xi_{i_1}^X) u_{j_1, j_2, j_3}$$

$$w_{i_1, i_2, j_3} = \sum_{j_2} \hat{\varphi}_{j_2}^{GL}(\xi_{i_2}^X) v_{i_1, j_2, j_3}$$

$$y_{i_1, i_2, i_3} = \sum_{j_3} \hat{\varphi}_{j_3}^{GL}(\xi_{i_3}^X) w_{i_1, i_2, j_3}$$

Fast matrix vector product with any points

$$(K_h)_{i,j} = \int_{\hat{K}} J_i DF_i^{-1} \mu DF_i^{*-1}(\xi_m) \hat{\nabla} \hat{\phi}_j^{GL} \cdot \hat{\nabla} \hat{\phi}_i^{GL} d\hat{x}$$

Fast matrix vector product with any points

$$(K_h)_{i,j} = \int_{\hat{K}} J_i DF_i^{-1} \mu DF_i^{*-1}(\xi_m) \hat{\nabla} \hat{\varphi}_j^{GL} \cdot \hat{\nabla} \hat{\varphi}_i^{GL} d\hat{x}$$

Matrix-vector product $K_h U$ can be split into three steps

$$v_m = \sum_j \hat{\nabla} \hat{\varphi}_j^{GL}(\xi_m^X) u_j$$

$$w_m = \omega_m J_i DF_i^{-1} \mu DF_i^{*-1} v_m$$

$$y_i = \sum_q \hat{\nabla} \hat{\varphi}_i^{GL}(\xi_m^X) w_m$$

Fast matrix vector product with any points

$$(K_h)_{i,j} = \int_{\hat{K}} J_i DF_i^{-1} \mu DF_i^{*-1}(\xi_m) \hat{\nabla} \hat{\varphi}_j^{GL} \cdot \hat{\nabla} \hat{\varphi}_i^{GL} d\hat{x}$$

Underlying factorization

$$\hat{S}_{i,j} = \hat{\nabla} \hat{\varphi}_i^{GL}(\xi_j^X)$$

$$(B_h)_m = \omega_m J_i DF_i^{-1} \mu DF_i^{*-1}$$

$$K_h = \hat{S} B_h \hat{S}^*$$

⇒ only storage of $J_i DF_i^{-1} \mu DF_i^{*-1}$

Fast matrix vector product with any points

By using the matrices

$$\hat{C}_{i,j} = \hat{\varphi}_i^{GL}(\xi_j^X)$$

$$\hat{S}_{i,j} = \hat{\nabla} \hat{\varphi}_i^{GL}(\xi_j^X)$$

$$\hat{R}_{i,j} = \hat{\nabla} \hat{\varphi}_i^X(\xi_j^X)$$

we have $\hat{S} = \hat{R}\hat{C}$

final matrix : $\hat{C}(-\omega^2 \mathbf{A}_h + \hat{R}\mathbf{B}_h\hat{R}^*)\hat{C}^*$

Fast matrix vector product with any points

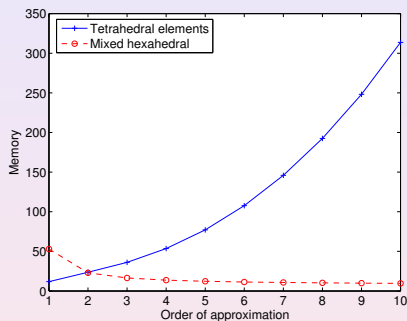
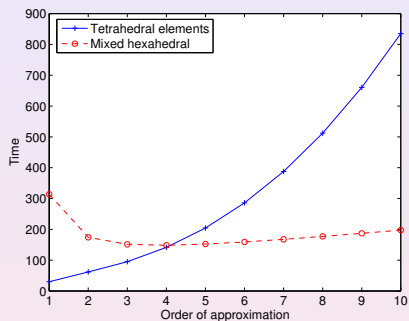
r is the order of approximation

For hexahedral elements (tensorization), complexity in $O(r^4)$

For tetrahedral elements (no tensorization), complexity in $O(r^6)$

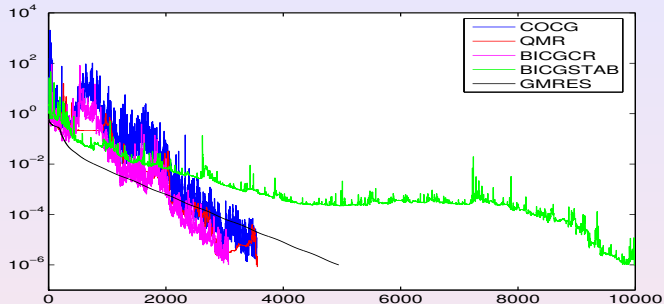
- If we use Gauss-Lobatto points to integrate : $\hat{C} = I$
- Same storage for Gauss or GL points
- Matrix-vector product slower with Gauss integration
- Loss of one order for GL points in 3-D

Matrix vector product faster than with tetrahedral ?



Comparison between hexahedral and tetrahedral elements, for computational time (left plot) and storage (right plot)

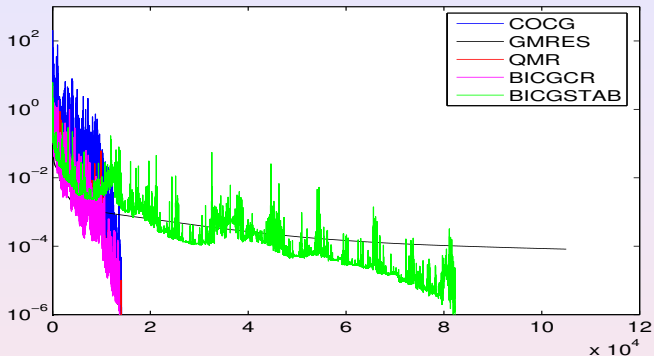
Iterative methods used



Evolution of the residual norm for the scattering of a perfectly conductor disc (Dirichlet condition).

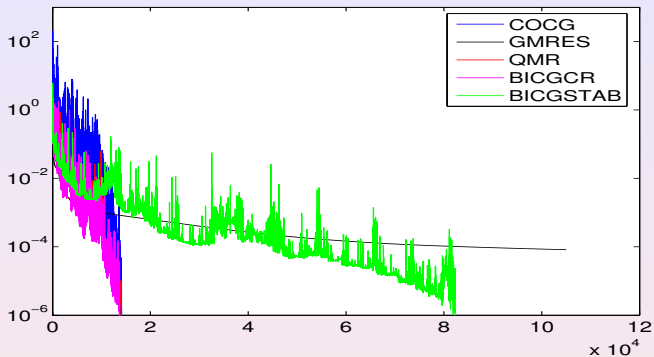
- GMRES, BICGSTAB and QMR for complex unsymmetric matrices
- COCG, BICGCR for complex symmetric matrices

Iterative methods used



Evolution of the residual norm for the scattering of a dielectric disc ($\rho = 4$).

Iterative methods used



- We choose to use BICGCR (faster) or COCG (less storage)
- Need of preconditioning techniques to have less iterations

- Incomplete factorization with threshold on the damped Helmholtz equation :

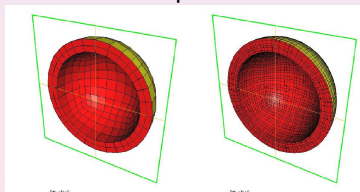
$$-k^2(\alpha + i\beta)\mathbf{u} - \Delta\mathbf{u} = 0$$

- see Y. Saad, Iterative methods for sparse linear systems

- Incomplete factorization with threshold on the damped Helmholtz equation :

$$-k^2(\alpha + i\beta)u - \Delta u = 0$$

- see Y. Saad, Iterative methods for sparse linear systems
- We use a Q_1 subdivided mesh to compute matrix



On the left, initial mesh Q_3 , on the right, subdivided mesh Q_1

- Incomplete factorization with threshold on the damped Helmholtz equation :

$$-k^2(\alpha + i\beta)\mathbf{u} - \Delta\mathbf{u} = 0$$

- see Y. Saad, Iterative methods for sparse linear systems
- Multigrid method on the damped Helmholtz equation
 - see Y. A. Erlangga and al, (Phd at Delft)

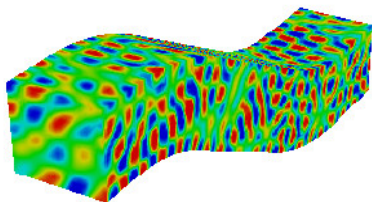
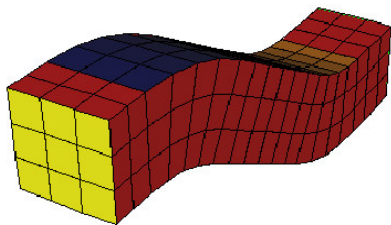
Preconditioning used

- Incomplete factorization with threshold on the damped Helmholtz equation :

$$-k^2(\alpha + i\beta)u - \Delta u = 0$$

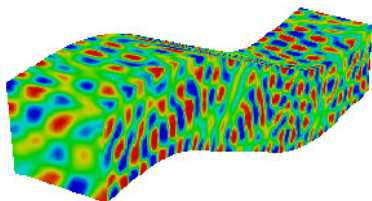
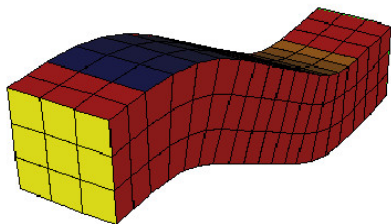
- see Y. Saad, Iterative methods for sparse linear systems
- Multigrid method on the damped Helmholtz equation
 - see Y. A. Erlangga and al, (Phd at Delft)
- Without damping, both preconditioners **do not lead** to convergence.
- A good choice of parameter is $\alpha = 1$, $\beta = 0.5$

Scattering by a cobra cavity



- Cobra cavity of length 20, and depth 4
- First order absorbing boundary condition on the yellow face

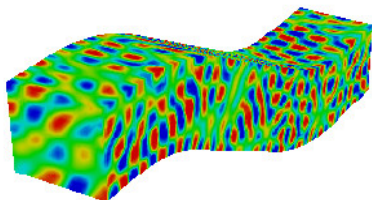
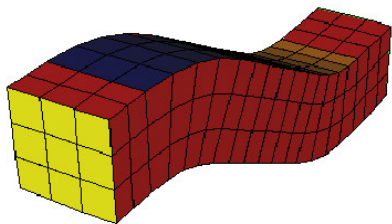
Scattering by a cobra cavity



Number of dofs to reach less than 5 % L^2 error

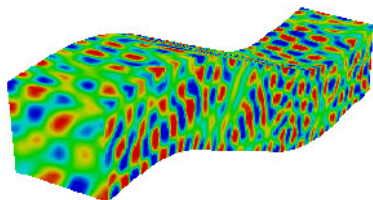
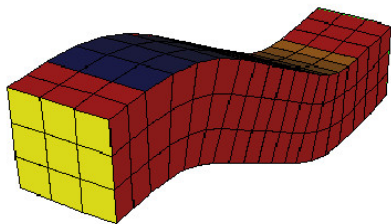
Order	struct \mathbf{Q}_4	struct \mathbf{Q}_6	struct \mathbf{Q}_8	n.s. \mathbf{Q}_4	n.s. \mathbf{Q}_6	n.s. \mathbf{P}_4
Nb dofs	330 000	185 000	95 600	567,000	466 000	360 000

Scattering by a cobra cavity



Finite element	structured \mathbf{Q}_8	non-structured \mathbf{Q}_6	non-structured \mathbf{P}_4
No preconditioning	9860 s	NC	NC
ILUT(0.01)	1021 s	13766 s	8036 s
Two-grid	1082 s	6821 s	14016 s

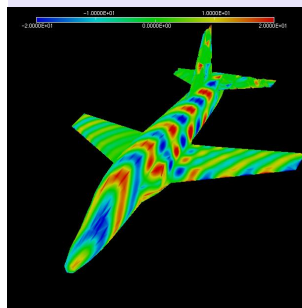
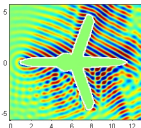
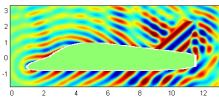
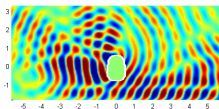
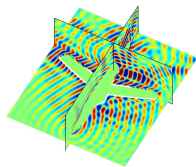
Scattering by a cobra cavity



Finite element	structured \mathbf{Q}_8	non-structured \mathbf{Q}_6	non-structured \mathbf{P}_4
No preconditioning	9 860 s	NC	NC
ILUT(0.01)	1 021 s	13 766 s	8 036 s
Two-grid	1 082 s	6 821 s	14 016 s

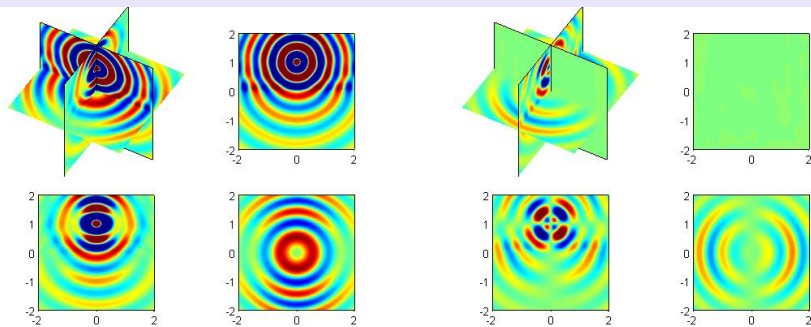
Finite element	structured \mathbf{Q}_8	non-structured \mathbf{Q}_6	non-structured \mathbf{P}_4
No preconditioning	32 Mo	162 Mo	251 Mo
ILUT(0.01)	150 Mo	1 250 Mo	1 400 Mo
Two-grid	60 Mo	283 Mo	710 Mo

Scattering by a plane



- Real part of the diffracted for an oblique incident plane wave
- Q4, 7.2 million of dofs (2 Go memory)
- 280 iterations and 2 hours with multigrid preconditioning
- More than 20 000 iterations without preconditioning

Time-harmonic elastic equation



- Displacement components u_x and u_z
- Q7, 4.3 million of dofs (with PML layers)
- 170 iterations and 50mn with multigrid preconditioning
- More than 20 000 iterations without preconditioning

Why do we choose Q_r for hexahedra ?

- P_r optimal finite element space for tetrahedra
- Is Q_r the right choice for hexahedra ? Why not choosing P_r (with DG method for instance) ?
- If transformation F_i is affine (i.e. **paralleloid**), P_r is the optimal finite element space
- If transformation F_i is trilinear (**general hexahedron**), Q_r is the optimal finite element space

Why do we choose Q_r for hexahedra ?

- P_r optimal finite element space for tetrahedra
- Is Q_r the right choice for hexahedra ? Why not choosing P_r (with DG method for instance) ?
- If transformation F_i is affine (i.e. **paralleloïd**), P_r is the optimal finite element space
- If transformation F_i is trilinear (**general hexahedron**), Q_r is the optimal finite element space

Condition of optimality

We define the finite element space with real element K_i :

$$V_h = \{u \in H^1(\Omega) \text{ such that } u|_{K_i} \in V_F^r\}$$

V_F^r : finite element space for the real element

We define the finite element space with reference element \hat{K} :

$$V_h = \{u \in H^1(\Omega) \text{ such that } u|_{K_i} \circ F_i \in \hat{V}^r\}$$

\hat{V}^r : finite element space for the reference element

Condition of optimality :

$$V_F^r \supset P_r$$

For hexahedra, we can prove :

$$V_F^r \supset P_r \Leftrightarrow \hat{V}^r \supset Q_r$$

Idea of the reason of optimality of Q_r

We consider a monomial of P_r :

$$x^m y^n z^p, \quad m + n + p \leq r$$

and we write its expression on reference element with transformation F_j :

$$x = a_1 + a_2 \hat{x} + a_3 \hat{y} + a_4 \hat{z} + a_5 \hat{x}\hat{z} + a_6 \hat{y}\hat{z} + a_7 \hat{x}\hat{y} + a_8 \hat{x}\hat{y}\hat{z}$$

$$y = b_1 + b_2 \hat{x} + b_3 \hat{y} + b_4 \hat{z} + b_5 \hat{x}\hat{z} + b_6 \hat{y}\hat{z} + b_7 \hat{x}\hat{y} + b_8 \hat{x}\hat{y}\hat{z}$$

$$z = c_1 + c_2 \hat{x} + c_3 \hat{y} + c_4 \hat{z} + c_5 \hat{x}\hat{z} + c_6 \hat{y}\hat{z} + c_7 \hat{x}\hat{y} + c_8 \hat{x}\hat{y}\hat{z}$$

By expanding $x^m y^n z^p$, the higher-degree term is equal to :

$$a_8^m b_8^n c_8^p \hat{x}^{m+n+p} \hat{y}^{m+n+p} \hat{z}^{m+n+p}$$

Hence we have obtained for $m + n + p = r$ the higher-degree term of Q_r .

Then, thanks to Bramble-Hilbert lemma, it is easy to get :

$$\|u - u_h\|_1 \leq Ch^r \|u\|_{r+1}$$

However, in our case, integrals are not evaluated exactly, we have to consider Strang Lemma :

$$\|u - u_h\|_1 \leq C \inf_{v_h \in V_h} \left\{ \|u - v_h\|_1 + \sup_{w_h \in V_h} \frac{|a(v_h, w_h) - a_h(v_h, w_h)|}{\|w_h\|_1} \right\}$$

Here we choose $v_h = \Pi_r u$ with the projector on real space, so that

$$v_h \in P_r \Rightarrow \hat{v}_h \in Q_r$$

$$\nabla v_h \in P_{r-1} \Rightarrow \widehat{\nabla v}_h \in Q_{r-1}$$

Thus, we are able to prove that :

$$(D - D_h)(v_h, w_h) = (D - D_h)(v_h - \pi_{r-1} v_h, w_h - \pi_0 w_h)$$

for Gauss rules, since $J_i \in Q_2$ (so $J_i \pi_{r-1} v_h w_h \in Q_{2r+1}$)

$$\Leftrightarrow |(D - D_h)(v_h, w_h)| \leq Ch^{r+1} \|v_h\|_r \|w_h\|_1$$

for Gauss-Lobatto rules

$$(D - D_h)(v_h, w_h) = (D - D_h)(v_h - \pi_{r-3} v_h, w_h - \pi_0 w_h)$$

$$\Leftrightarrow |(D - D_h)(v_h, w_h)| \leq Ch^{r-1} \|v_h\|_{r-2} \|w_h\|_1$$

Therefore, we have a loss of order for Gauss-Lobatto rules

Quadrature error

For stiffness term, we have :

$$(K - K_h)(v_h, w_h) = (D - D_h)(\nabla v_h - \pi_r \nabla v_h, \nabla w_h)$$

for Gauss rules, since $J_i DF_i^{*-1} \hat{\nabla} \hat{w}_h \in Q_{r+1}$

$$\Leftrightarrow |(K - K_h)(v_h, w_h)| \leq Ch^{r+1} \|v_h\|_{r+1} \|w_h\|_1$$

for Gauss-Lobatto rules

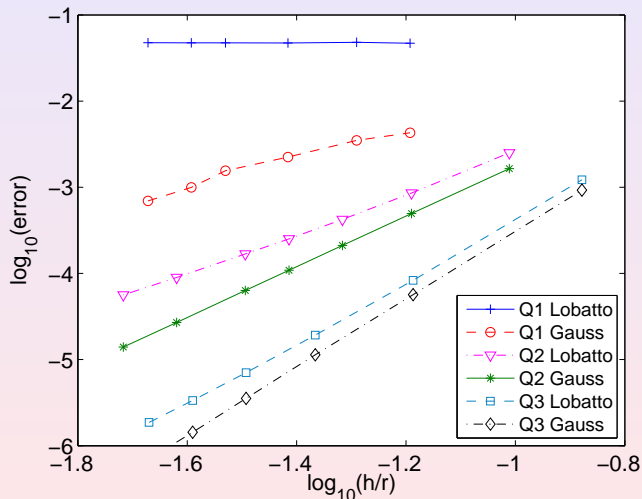
$$(K - K_h)(v_h, w_h) = (D - D_h)(\nabla v_h - \pi_{r-2} \nabla v_h, \nabla w_h)$$

$$\Leftrightarrow |(D - D_h)(v_h, w_h)| \leq Ch^{r-1} \|v_h\|_{r-1} \|w_h\|_1$$

Therefore, we have a loss of order for Gauss-Lobatto rules

Quadrature error

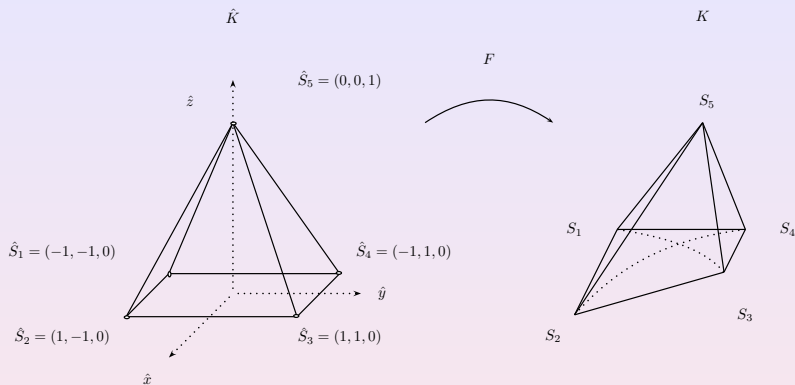
Illustration of this effect for a cube meshed with split tetrahedra



Why pyramids ?

- Automatic generation of high-quality hexahedral meshes is difficult
- “Solution of split tetrahedra” is not interesting
- Some mesh tools are able to produce meshes with a high ratio of hexahedra and some remaining pyramids/tets/prisms.
- Pyramids elements not as well known as other elements.

Two main approaches



Simplest expression of F_i (Bedrosian) :

$$F_i(\hat{x}, \hat{y}, \hat{z}) = A + B\hat{x} + C\hat{y} + D\hat{z} + \frac{\hat{x}\hat{y}}{4(1 - \hat{z})} (S_1 + S_3 - S_2 - S_4)$$

Two main approaches

- Use of rational fractions to define F_i
 - Early work of [Bedrosian](#) with explicit first and second order basis functions
 - Work of [Sherwin, Karniadakis, Warburton](#) : h-p Basis functions obtained by considering a degenerated cube (coincidence with Bedrosian functions for $r = 1$)
 - Recent work of [Nigam, Phillips](#) with a reference infinite pyramid (but same basis functions as Bedrosian for $r = 1$)
- Use of piecewise polynomial to define F_i (polynomial on each sub-tetrahedron)
 - Work of [Wieners](#), with first and second order basis functions
 - Work of [Knabner and Summ](#), with an analysis of this transformation
 - Work of [Bluck and Walker](#), with a proposition of high order basis functions

Optimal finite element space

Same approach than for hexahedra : We consider a monomial of P_r :

$$x^m, \quad m \leq r$$

$$(a + b\hat{x} + c\hat{y} + d\hat{z} + \alpha(\frac{\hat{x}\hat{y}}{1-\hat{z}}))^m$$

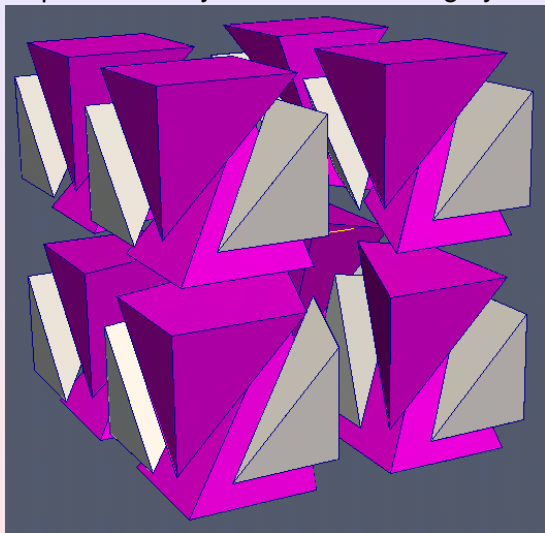
$$\sum_k C_m^k (a + b\hat{x} + c\hat{y})^k (d\hat{z})^k \alpha^{m-k} (\frac{\hat{x}\hat{y}}{1-\hat{z}})^{m-k}$$

After some calculations, you can show that the optimal finite element space is

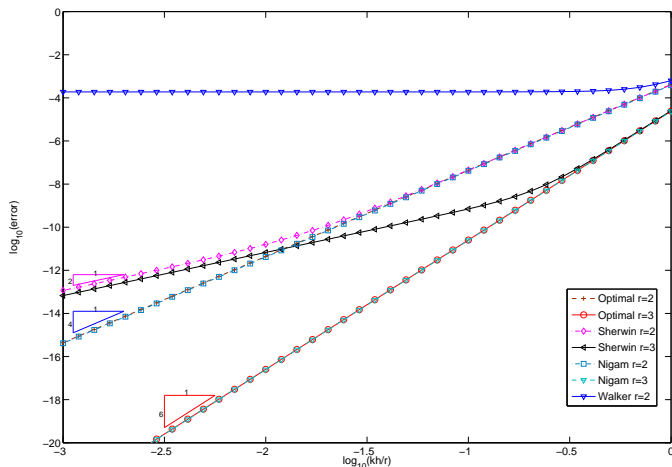
$$\hat{V}^r = P_r \oplus \sum_{k=0}^{r-1} (\frac{\hat{x}\hat{y}}{1-\hat{z}})^{r-k} P_k(\hat{x}, \hat{y})$$

Numerical comparison between different methods

We perform a dispersion analysis on the following hybrid mesh :



Numerical comparison between different methods



Numerical comparison between different methods

- We obtained same finite element space as [Demkowicz/Zaglmayr](#)
- We obtained a smaller finite element space than [Nigam/Phillips](#)
- We proposed modifications of basis functions of [Sherwin/Karniadakis/Warburton](#) so that they span the optimal finite element space
- Alternative approach using piecewise polynomial (by splitting pyramid in two or four tets) is not consistent for non-affine pyramids

Influence of quadrature

Then, thanks to Bramble-Hilbert lemma, it is easy to get :

$$\|u - u_h\|_1 \leq Ch^r \|u\|_{r+1}$$

However, in our case, integrals are not evaluated exactly, we have to consider Strang Lemma :

$$\|u - u_h\|_1 \leq C \inf_{v_h \in V_h} \{ \|u - v_h\|_1 + \sup_{w_h \in V_h} \frac{a(v_h, w_h) - a_h(v_h, w_h)}{\|w_h\|_1} \}$$

Here we choose $v_h = \Pi_r u$ with the projector on real space, so that

$$v_h \in P_r \Rightarrow \hat{v}_h \in \hat{V}^r$$

$$\nabla v_h \in P_{r-1} \Rightarrow \widehat{\nabla v}_h \in \hat{V}^{r-1}$$

By expressing integrals on the cube, we are able to prove that :

$$(D - D_h)(v_h, w_h) = (D - D_h)(v_h - \pi_r v_h, w_h - \pi_0 w_h)$$

for Gauss-Jacobi rules (because of $(1 - \hat{z})^2$ weight), since $J_i \in Q_1$ (so $J_i \pi_r v_h w_h \in Q_{2r+1}$)

$$\Leftrightarrow |(D - D_h)(v_h, w_h)| \leq Ch^{r+2} \|v_h\|_{r+1} \|w_h\|_1$$

We could use Gauss-Jacobi-Lobatto rules for mass term without loss of accuracy

For stiffness term, we have :

$$(K - K_h)(v_h, w_h) = (D - D_h)(\nabla v_h - \pi_r \nabla v_h, \nabla w_h)$$

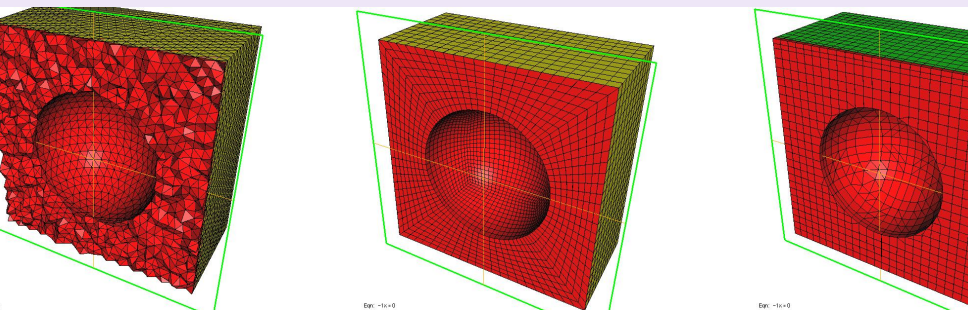
for Gauss rules, since $J_i DF_i^{*-1} \hat{\nabla} \hat{w}_h \in Q_{r+1}$

$$\Leftrightarrow |(K - K_h)(v_h, w_h)| \leq Ch^{r+1} \|v_h\|_{r+1} \|w_h\|_1$$

we can't use Gauss-Jacobi-Lobatto rules without loss of an order

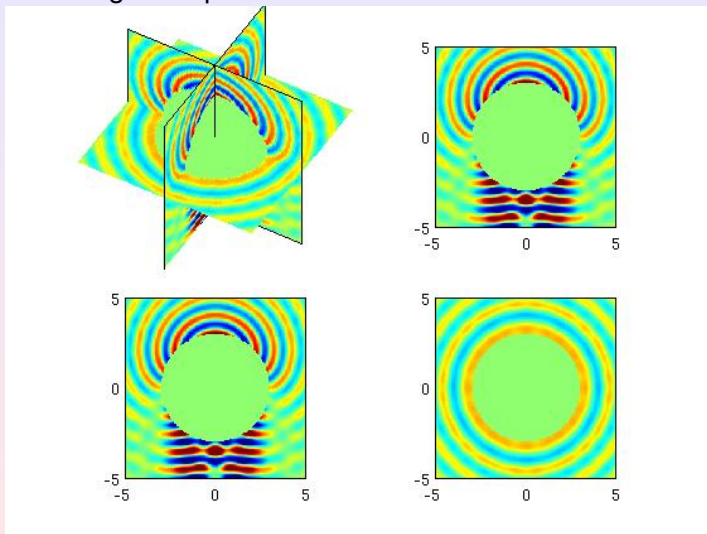
Numerical results for Helmholtz equation

Comparison of three kind of meshes :



Numerical results for Helmholtz equation

For the scattering of a sphere :



Numerical results for Helmholtz equation

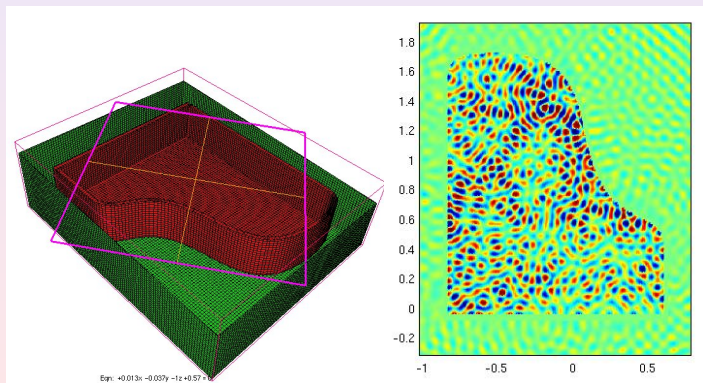
For order 4 for tets, and order 5 for hex/hybrid, less than 2 % error :

Mesh type	Tetra	Hexa	Split Tetra	Hybrid
number of dofs	339 000	315 000	520 000	266 000
multigrid prec.	119 iter (587s)	130 iter (152s)	93 iter (266s)	128 iter (161s)

Numerical results for wave equation

Use of Discontinuous Galerkin formulation for solving wave equation :

$$\frac{\partial^2 u}{\partial t^2} - \Delta u = 0$$



Numerical results for wave equation

Efficiency of different kind of meshes for the piano-shaped cavity with a third order approximation on a fine mesh :

Mesh type	Tetra	Split Tetra	Hybrid
Obtained accuracy	5.7%	9.4 %	6.3%
Number of dofs	16.9 millions	49.3 millions	14.9 millions
Time step (freq = 14)	$\Delta t = 0.0004$	$\Delta t = 0.0002$	$\Delta t = 0.0005$
Computational time	4.3 days	12.3 days	1.2 day

Computational time obtained by summing computational time for each processor without cost of communications.